Durham University

Durham Research Online

Deposited in DRO:

13 February 2018

Version of attached file:

Accepted Version

Peer-review status of attached file:

Peer-reviewed

Citation for published item:

Kennedy, Stuart R. and Jones, Christopher D. and Yufit, Dimitrii S. and Nicholson, Catherine Emma and Cooper, Sharon J. and Steed, Jonathan W. (2018) 'Tailored supramolecular gel and microemulsion crystallization strategies – is isoniazid really monomorphic?', CrystEngComm., 20 (10). pp. 1390-1398.

Further information on publisher's website:

https://doi.org/10.1039/C8CE00066B

Publisher's copyright statement:

Additional information:

Use policy

The full-text may be used and/or reproduced, and given to third parties in any format or medium, without prior permission or charge, for personal research or study, educational, or not-for-profit purposes provided that:

- a full bibliographic reference is made to the original source
- a link is made to the metadata record in DRO
- the full-text is not changed in any way

The full-text must not be sold in any format or medium without the formal permission of the copyright holders.

Please consult the full DRO policy for further details.

Durham University Library, Stockton Road, Durham DH1 3LY, United Kingdom
Tel : +44 (0)191 334 3042 | Fax : +44 (0)191 334 2971
https://dro.dur.ac.uk

Journal Name

RSCPublishing

COMMUNICATION

Tailored Supramolecular Gel and Microemulsion Crystallization Strategies – is Isoniazid Really Monomorphic?†

Cite this: DOI: 10.1039/xoxxoooooox

Received ooth January 2012,
Accepted ooth January 2012

DOI: 10.1039/xoxxoooooox

www.rsc.org/

Stuart R. Kennedy[a], Christopher D. Jones[a], Dmitry S. Yufit[a], Catherine E. Nicholson[b], Sharon J. Cooper[a] and Jonathan W. Steed*[a]

We report the application of supramolecular gel and microemulsion droplet crystallisation methodologies to isoniazid crystallization. Tailored gelators have been designed with isoniazid mimetic functionality in an attempt to control crystal morphology and polymorphic behaviour. Microemulsion crystallisation was investigated to achieve thermodynamic control over drug crystallisation. Both techniques resulted in only a single form of isoniazid implying that it is genuinely monomorphic.

Walter McCrone once famously stated "every compound has different polymorphic forms, and that, in general, the number of forms known for a given compound is proportional to the time and money spent in research on that compound".[1] This prediction is apparently supported by the large number of yet unobserved crystal forms calculated to be of similar energy to the experimentally isolated polymorphs in many computational crystal structure calculation polymorph landscapes.[2] However among compounds that have undergone extensive polymorph screening only around 36 % are found to be polymorphic. This figure rises to 57 % when solvates are included.[3] Is it the case that modern polymorph screening methods simply do not address the chemical space in which these 'missing' solid forms can nucleate and grow, or is it true that, contrary to McCrone's instinct, some compounds are always destined to exhibit just a single crystal form?

Isoniazid (or isonicotinic acid hydrazine) is a well-known front-line drug in the treatment of tuberculosis.[4, 5] The first crystal structure determination of isoniazid was reported by Jensen[6] who described the formation of needle-shaped crystals grown from ethanol. Further more recent redeterminations at lower temperature have been reported.[7-9] To date isoniazid is not known to exhibit polymorphic behaviour.[10] It does, however, form an interesting range of co-crystals including materials incorporating other pharmaceutically active substances which can improve the physiochemical properties of the drug or even act as a combined therapy.[8, 10-17] This tendency to form co-crystals suggests that the known single–component structure of isoniazid is perhaps not overwhelmingly favoured and hence the monomorphic isoniazid represents an interesting target for unconventional crystallization methodologies.

The use of low molecular weight gels (LMWG) as media to template or influence crystal growth is a potentially powerful new method for polymorph screening and crystal morphology modification.[18-25] Gelators can be designed to form gels in a variety of solvent systems and the reversibility of gelation by small molecules offers a convenient way to isolate gel-grown pharmaceutical crystals. There are numerous examples of compounds acting as LMWG such as fatty acids, steroids, anthryl derivatives, amino acids or metal-based gels.[26-33] Among the most versatile are urea-based gelators due to the relative ease of designing and synthesising tailor-made gelators with targeted solubility and chemical functionality than can complement a particular drug functional group or fragment.[20, 34] Bis(urea) gelators are relatively simple to prepare from the reaction of an isocyanate with an amine allowing facile access to a wide range of bis and tris(urea)s with a variety of spacers and functional groups.[35-37] Recently we have demonstrated how LMWG can be used for pharmaceutical crystal growth by designing molecules with both gel forming attributes and either generic or drug mimetic functionality. Careful consideration of both solvent and gelator has been shown to yield differing crystal forms of the same drug molecule.[18, 20] Gels with drug-mimetic functionality offer the possibility of significant interactions between drug and gel fibre surface and even epitaxial overgrowth of the drug crystal on the gel parent. Unusual gels such as a nanocellulose organogel have also revealed previously unknown solid forms.[22]

In addition to gel methodologies, an emerging crystallization technique is crystallization in microemulsion droplets.[38-41] Microemulsion crystallisation allows for thermodynamic control over crystallisation outcome, essentially 'leapfrogging' Ostwald's rule of stages.[41] Between them, supramolecular gels and microemulsions offer the possibility of

significantly expanding polymorph discovery space with the locally order gel fibre surface offering the possibility of epitaxial overgrowth of hard-to-nucleate metastable polymorphs, while the microemulsion approach 'zeroes-in' on the thermodynamic form.

In the present work we report a tailored supramolecular gel phase approach to search for isoniazid polymorphs and compare the outcome to the microemulsion method and to conventional solution crystallization which has been known to give rise to just one pure form of isoniazid since 1954.[6]

Gelator design and synthesis

Hydrogelators bearing an isoniazid-derived functionality have previously been reported,[42] but have not been studied in a pharmaceutical crystallization context. Synthesis of the isoniazid-mimetic gelators **1** and **2** (Figure 1) was carried out in good yield by the relatively straightforward one-pot reaction between isoniazid and the desired isocyanate (see experimental section). The diphenylmethane derived spacer in compound **1** commonly results in highly effective gelation behaviour in bis(urea)s, while the sterically confined spacer in **2** tends to result in a mixture of crystalline and gel-forming behaviour.[43, 44]

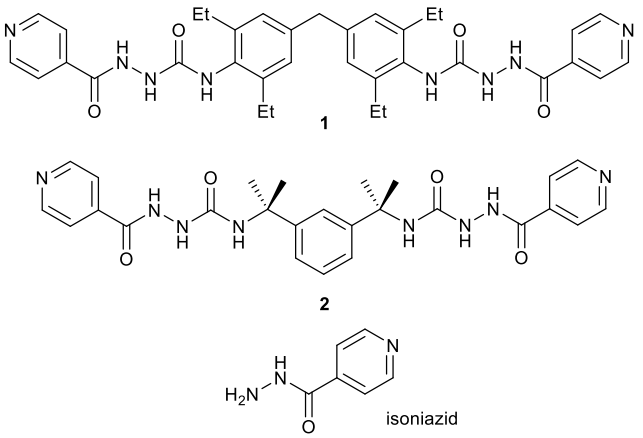

Figure 1. Molecular structures of isoniazid and isoniazid-mimetic gelators **1** and **2**.

Gelation

Compounds **1** and **2** were screened for gelation behaviour in a range of common solvents. All gelation tests were carried out at 1 % w/v by heating a sample (5 mg) suspended in the desired solvent (0.5 mL) followed by sonication[45] for 60 seconds. Gelation experiments of compound **1** were carried out in 51 solvents (Table S1, supplementary information). The gelator dissolved in 27 of these 51 solvents and gels formed in 19 of these 27 samples. In 10 of these gelled samples were opaque while the remaining 9 gave more transparent gels. In most cases gelation occurs rapidly and the mixture forms gels prior to the end of the sonication cycle. A selection of the transparent gels was dried by allowing the solvent to slowly evaporate over two days and the resulting xerogels imaged using SEM (Figure 2). The SEM micrographs of the xerogels of **1** from various solvents show that there is a fibrous network present and in some cases helical fibres are observed (Figure 2a). Compound **2** proved to be a non-gelator but was soluble in 34 of the 51 solvents tested and crystallized from six of them (*vide infra*).

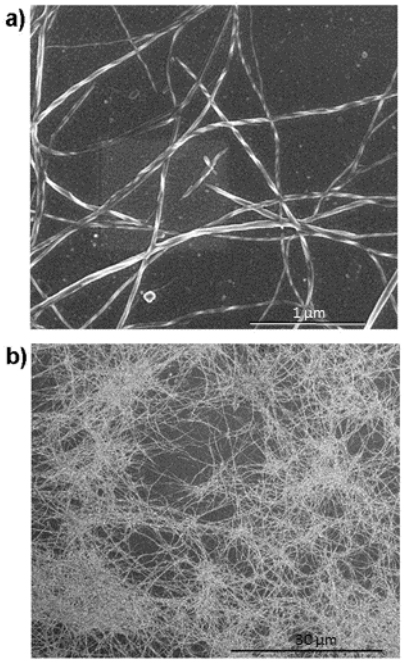

Figure 2. SEM images of xerogels of compound **1**. a) Dried dimethyl formamide gel showing helical fibres. b) Fibrous network from dimethyl acetamide showing the relatively long length of some of the individual fibres. In both cases the gels investigated were transparent where the samples were air dried for two days and coated with 3 nm of chromium.

Gel phase crystallisation of isoniazid

Crystallization tests were carried out for isoniazid in the 19 solvents in which gels were obtained for gelator **1** using a 1 wt% isoniazid. The drug substance and gelator were warmed to give a solution and then allowed to cool on the benchtop resulting in gelation over periods of 1 – 24 h. Crystallization had occurred in a total of eight samples after one week in the sealed vials at room temperature. All eight samples proved to be the known polymorph of isoniazid. In six of the eight cases the crystals adopted the same needle-shaped morphology as the material from solution control experiments. Some differences were observed for nitrobenzene and propan-1-ol, however. When isoniazid was introduced to a nitrobenzene solution containing gelator **1** and allowed to gel, crystal growth proved to be significantly slower than in a solution control experiment without gelator under the same conditions and there was no evidence of crystalline material after a few hours. Over 48 hours however, a single large plate-shaped crystal appeared, consistent with the reduced nucleation and convection within the gel (Figure 3). Interestingly, after 96 hours the typically very stable nitrobenzene gel of **1** had collapsed. It is evident that the presence of isoniazid within this gel seems to affect its stability. This slow reversal of the gelation process is potentially advantageous as it allows for the easy removal of the crystal without the need of potentially damaging it using other removal techniques (*e.g.* the introduction of competitor species such as anions to dissolve the gel).[18, 46, 47] An additional benefit of this 'collapsing' gel is the potential to recycle the gelator to undertake further crystal growth in the same sample by removing isoniazid crystals by filtration and subsequently thermally reinitiating the gel formation process in the presence of further drug. Single crystal X-ray diffraction experiments carried out on the gel-grown isoniazid crystal showed it is also the previously reported polymorph despite its different morphology.[6-8]

 This journal is © The Royal Society of Chemistry 2012

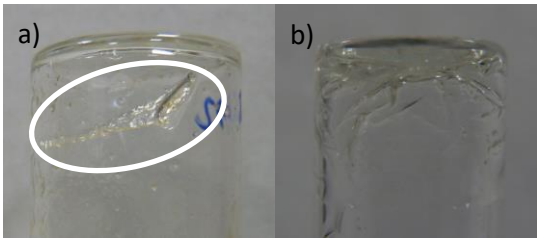

Figure 3. a) Single sample-spanning isoniazid crystal obtained after the collapse of a nitrobenzene gel of **1**. b) Relatively small needle-shaped crystals of isoniazid obtained from nitrobenzene in the absence of gel.

Using gels as crystal growth media not only has the potential to affect crystal size but can also alter crystal morphology. Isoniazid itself does not crystallise from propan-1-ol however, when isoniazid was introduced into a 1 wt% sample of propan-1-ol containing the gelator **1**, the formation of crystalline material was observed after 1 week. The crystals adopted a small block-shaped morphology (Figure 4). Again this material proved to be the known polymorph of isoniazid.[6-8]

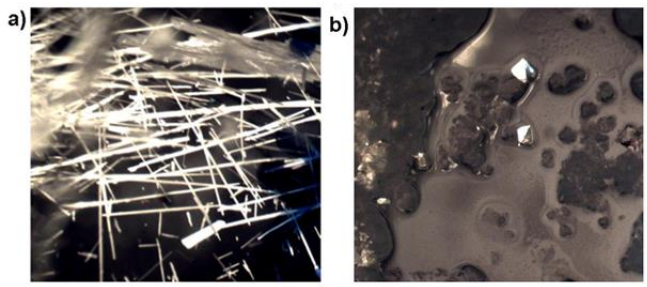

Figure 4. a) Typical needle-shaped isoniazid crystals grown from methanol. b) Isoniazid crystals grown in a propan-1-ol gel of **1** showing a clear change in crystal habit. Isoniazid does not crystallize from propan-1-ol in the absence of gel.

Microemulsion crystallisation of isoniazid

Crystallization in microemulsion droplets leads to thermodynamic control under supersaturation conditions where crystallization is only just achievable. At supersaturations below this, the supersaturated system is stabilised due to the nanoconfinement and at supersaturations significantly above this, the crystallization reverts to the kinetic control typically observed in bulk systems.[39-41] Since both conventional crystallization and gel-phase experiments result only in a single solid form of isoniazid, microemulsion crystallization represents a way to further test whether this form is highly kinetically favoured or whether it does indeed represent a 'thermodynamic sink'. In each microemulsion experiment, 2 × 2 g aliquots of sodium dioctyl sulfosuccinate (AOT) solutions in heptane at 3, 10, 20 and 25% AOT by mass were combined with 25 µl or 100 µl of a 38 mg mL^{-1} aqueous solution of isoniazid using a micropippete. The microemulsions were shaken by hand to form an optically transparent single phase and held at 21 °C. Isoniazid is undersaturated in bulk aqueous solutions at 38 mg mL^{-1} but becomes supersaturated in the microemulsion droplet core due to preferential water adsorption at the surfactant interface.

In the microemulsions containing 100 µL isoniazid solution, needle-shaped crystals were obtained after 3 days in all systems. Needles were also obtained after 3 days in the 3 and 10% AOT microemulsions containing 25 µL isoniazid solution. In all cases, XRD and melting point data established that the crystals were the known form of isoniazid. No crystallization occurred for the smaller droplet microemulsions containing 20 and 25% AOT and 25 µL isoniazid solution, even after one year. The smaller the droplet size, the higher the supersaturation required to achieve crystallisation because the supersaturation is rapidly depleted as the crystal nucleus grows. Hence, these systems were stabilised due to nanoconfinement because this supersaturation threshold was not achieved. The microemulsions chosen spanned a range of sizes from too small for crystallization to occur (25 µL isoniazid solution in 20 and 25% AOT solution) to larger droplet sizes (100 µL isoniazid solution in 3 and 10% AOT solution) where kinetic forms would crystallize. The fact that all microemulsions that were capable of forming crystals yielded the known form reinforces the hypothesis that isoniazid is monomorphic.

Solid state chemistry of compound 2

While the relatively bulky spacer in **2** limits its ability to form hydrogen bonded tapes, and hence form gels. As a result its higher crystallinity allows the characterisation of a number of solvates that collectively give insight into the intermolecular interactions in the gels. Crystallization of **2** from six different solvent systems by slow cooling followed by slow evaporation of the cooled solution resulted in a non-solvated form and five solvates with water, propan-2-ol, butan-1-ol, cyclohexanone and 4-ethylpyridine which were all characterised by X-ray crystallography.

*Non-solvated structure of **2***

Crystals of **2** grown from propan-1-ol proved to be non-solvated and adopt a high symmetry tetragonal cell with the space group $I\bar{4}2d$. The asymmetric unit comprises one half molecule of **2** ($Z' = 0.5$[48]). A combination of the sterically demanding spacer and competing hydrogen bonding interactions, prevent urea tape formation (Figure 5). The NH groups from the isoniazid mimetic part of **2** results in the formation of a type I hydrogen-bonded synthon (Figure 6) involving a combination of a $\boldsymbol{R_2^2}(10)$ hydrogen bonded ring and the urea-pyridine $\boldsymbol{R_2^1}(6)$ synthon.[49, 50] The $\boldsymbol{R_2^2}(10)$ motif takes advantage of the less sterically hindered side of the carbonyl acceptor and might potentially allow hydrogen bonded tape aggregation and hence gelation, the chain is truncated by the $\boldsymbol{R_2^1}(6)$ pyridyl interaction which is not typical in gels[50] and likely inhibits fibre formation.[34]

*Solvate structures of **2***

Solvate structures of **2** with water, propan-2-ol, butan-1-ol and cyclohexanone were also characterised by X-ray crystallography. In the monohydrate structure **2**·H_2O the crystals form a conglomerate[51] in the Sohnke space group $P2_12_12_1$ with $Z' = 1$ despite the achirality of the molecule. The propan-2-ol structure is a centrosymmetric disolvate of **2**· in *Pbca* with $Z' = 1$. The cyclohexanone disolvate is also centrosymmetric, **2**·2 cyclohexanone $P2_1/c$ with $Z' = 2$. Finally, the 2-butanol monosolvate (**2**·butan-1-ol) is a more unusual $Z' = 4$ in $P\bar{1}$.

In all four solvated structures the urea α-tape that is generally thought to be responsible for gel formation[52, 53] is sterically unfavourable and is replaced by varying types of alternative hydrogen bonding synthons. For **2**·H_2O, the water molecule non-covalently bridges together the carbonyl group of the isoniazid-derived part of the molecule with a urea NH proton thereby preventing fibre and subsequent gel formation (Figure 7). Additionally, the formation of a NH•••N pyridyl-urea hydrogen-bonded synthon at the other urea group and the formation of an $\boldsymbol{R_2^2}(10)$ synthon between the drug mimetic part of one molecule and a urea carbonyl of another molecule, further inhibit urea tape formation (Type II hydrogen bonding motif, Figure 6).

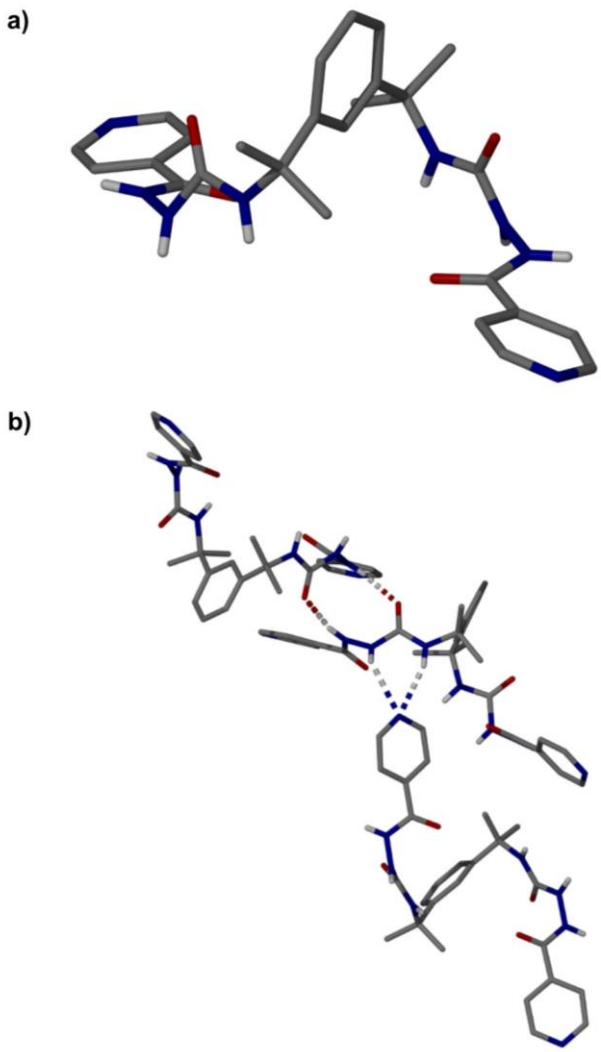

Figure 5. a) Molecular structure of **2**. b) Type I hydrogen bonding synthon observed in the extended structure of **2**. CH hydrogen atoms omitted for clarity.

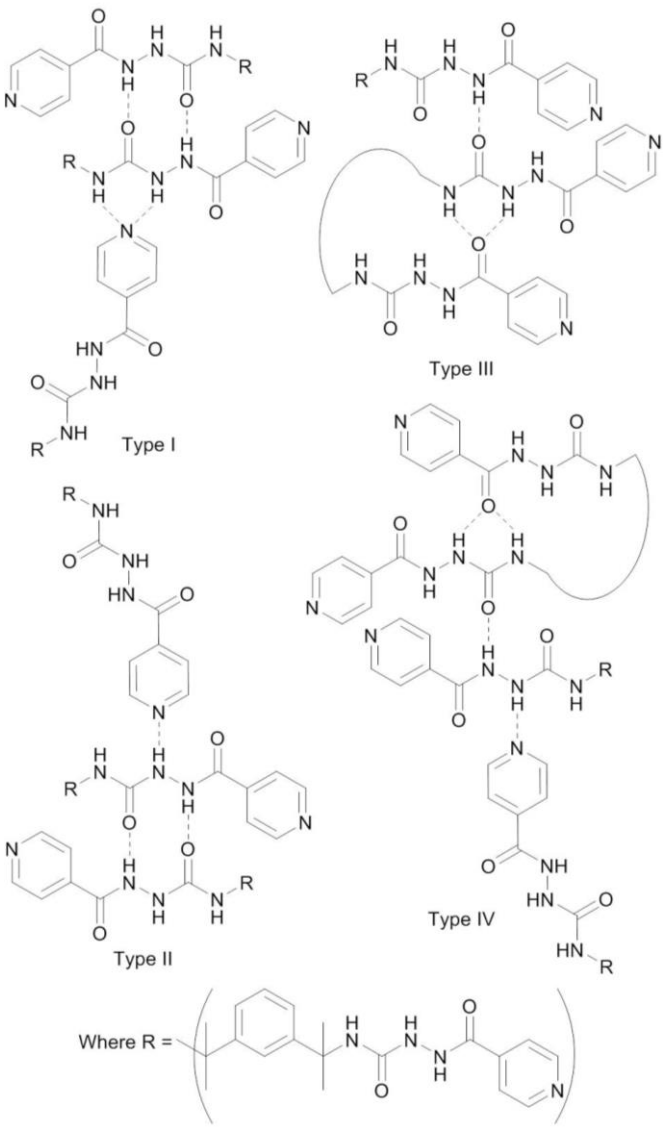

Figure 6. Hydrogen-bonded synthons observed in the solvated and non-solvated crystal structures of **2**. Type I comprises both a $\boldsymbol{R_2^1}(6)$ NH•••N pyridyl-urea hydrogen-bonded synthon and a $\boldsymbol{R_2^2}(10)$ NH•••O urea-isoniazid mimetic hydrogen-bonded synthon. Type II comprises both a pyridyl hydrogen bonding to a single urea proton and a $\boldsymbol{R_2^2}(10)$ NH•••O urea-isoniazid mimetic hydrogen-bonded synthon. Type III intramolecular formation of a $\boldsymbol{S_2^1}(6)$ NH•••O urea-carbonyl hydrogen-bonded synthon. Type IV intramolecular formation of a $\boldsymbol{S_2^1}(6)$ NH•••O urea-carbonyl hydrogen-bonded synthon along with a NH•••N urea-pyridyl hydrogen-bonded synthon.

This journal is © The Royal Society of Chemistry 2012

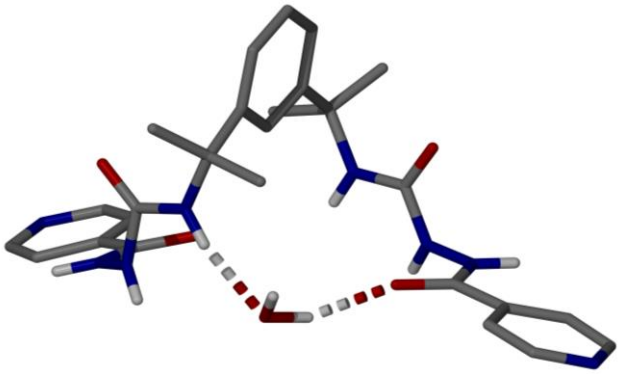

Figure 7. The asymmetric unit of **2**·H_2O showing the water molecule bridging the isoniazid mimetic part of **2** with a urea NH group. CH hydrogen atoms are omitted for clarity.

In the crystal structure of **2**·2 propan-2-ol an $\boldsymbol{S_2^1}(6)$ hydrogen-bonded synthon between the carbonyl of the drug mimetic part of **2** and a urea group prevent α-tape formation (Type III hydrogen bonding motif), Figure 8. Additional NH•••O urea-carbonyl intramolecular and NH•••O intermolecular hydrogen bonding interactions further disrupts urea-tape formation. Unlike the Type I and Type II hydrogen-bonded synthons, there are no pyridyl-urea interactions in **2**·2 propan-2-ol due the presence OH•••N pyridyl-solvent interactions.

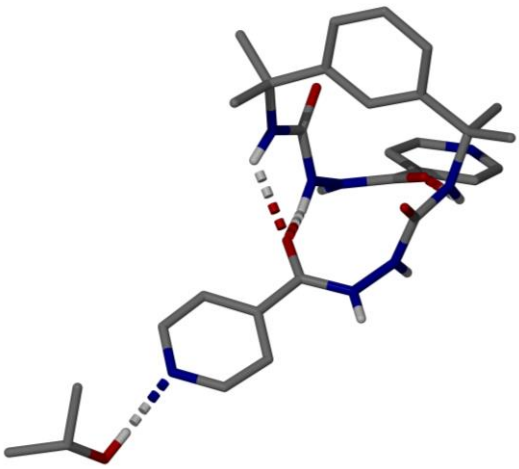

Figure 8. Part of the asymmetric unit of **2**·2 propan-2-ol showing the intramolecular hydrogen bonded folding of the molecule. CH hydrogen atoms are omitted for clarity.

The crystal structure of **2**·2 cyclohexanone is based on type III hydrogen bonding synthons (Figure 6). A cyclohexanone molecule bridges the urea groups via NH•••O urea-solvent hydrogen bonding interactions as an alternative to urea tape formation (Figure 9). Intramolecular NH•••O interactions are present between a urea hydrogen atom and the carbonyl of the isoniazid mimetic part of the molecule. The presence of $\boldsymbol{R_2^2}(10)$ hydrogen bonding interactions between the NH group on the drug mimetic region and urea carbonyl groups also replace urea tape formation.

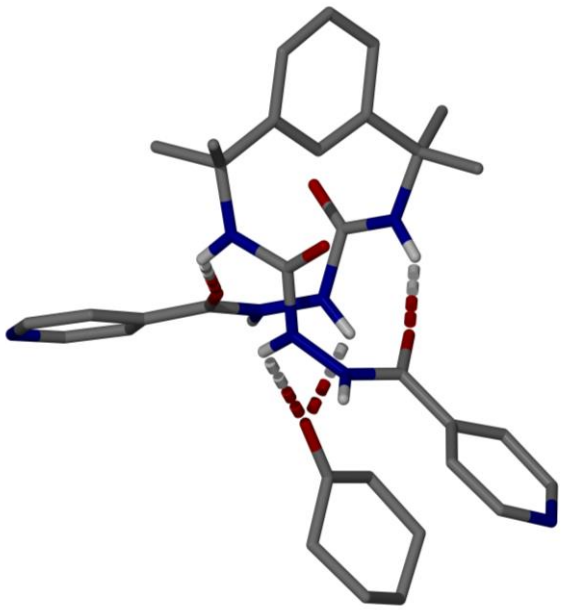

Figure 9. Part of the asymmetric unit of **2**·2 cyclohexanone showing both intramolecular and solvent hydrogen bonding. CH hydrogen atoms are omitted for clarity.

The crystals of **2**·butan-1-ol, were found to be weakly diffracting and the structure was determined using synchrotron radiation at the I19 facility at Diamond, UK. Disorder is present in two solvent molecules and one of the molecules of **2**. In three of the crystallographically independent molecules of **2**, the urea groups form a type IV hydrogen-bonding synthon to give a supramolecular dimer (Figure 10). Assembly of the dimer is via $\boldsymbol{S_2^1}(6)$ NH···O urea-carbonyl and NH···N urea-pyridyl hydrogen-bonded synthons along with a π-stacking interaction between the isoniazid mimetic tails. The fourth independent molecule of **2** forms a type III hydrogen-bonded synthon.

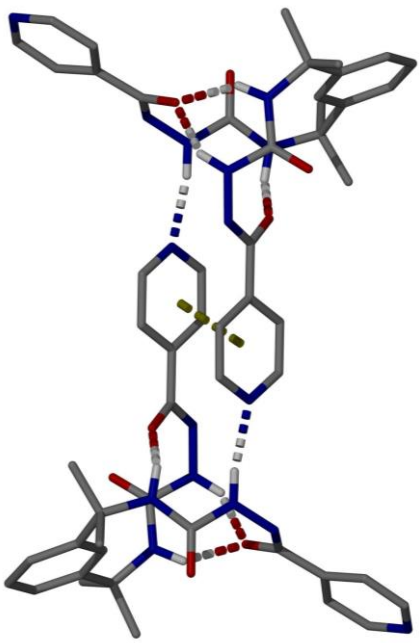

Figure 10. Illustration of part of the $Z' = 4$ asymmetric unit observed in **2**·butan-1-ol showing intramolecular and intermolecular hydrogen bonding interactions. The π-stacking interaction present in the dimer

is highlighted as a yellow dashed line. Hydrogen atoms except those involved in hydrogen bonding interactions are omitted for clarity.

*Drug-like co-crystallisation of **2** with 4-Ethylpyridine*

While there have been a number of reports of drug substances crystallized in small-molecule gels,[18-24, 34, 54] it is perhaps surprisingly that there have been no reports of drug-gelator co-crystals. The main reason for this paucity is likely to be time-resolved self-sorting in which gelation by gelator aggregation occurs more quickly than the formation of any putative cocrystals. While such self-sorting is important in the application of LMWG to drug crystallization, structural characterisation of a gelator-drug cocrystal would give useful insight into the way in which a drug may interact with a gel surface and hence allow for a greater understanding of the drug-gelator interactions which may be the beginnings of drug crystal nucleation in supramolecular gels. In order to obtain such structural insight we investigated different crystallisation techniques with a view to forming a co-crystal of **2** with isoniazid and with the related pharmaceutical compounds 4-aminopyridine and the liquid drug-like model compound 4-ethylpyridine. Co-crystallization was attempted by melting isoniazid, adding varying amounts of **2** and allowing the melt to cool to room temperature. However single crystal analysis on a number of samples showed that only the known form of isoniazid was isolated. Co-crystallization with 4-aminopyridine was similarly unsuccessful. However, 1:1 cocrystals of **2** with 4-ethylpyridine were obtained by allowing a hot solution of **2** in 4-ethylpyridine (m.p. 2.4 °C) to cool to room temperature. The asymmetric unit comprises two molecules of **2** and two molecules of 4-ethylpyridine. The structure comprises $\boldsymbol{S}_2^1(6)$ NH···O urea-carbonyl hydrogen bonding interactions (type IV hydrogen-bonded synthon, Figure 6). The structure also incorporates $\boldsymbol{R}_2^2(10)$ NH···O hydrogen bonding interactions between the isoniazid mimetic NH group and urea carbonyl group and as in the other structures of **2**, no urea α-tape $\boldsymbol{R}_2^1(6)$ type interactions are observed (Figure 11). Several molecules of **2** encapsulate two molecules of 4-ethylpyridine completely isolating the guest molecules from other solvent (Figure 12). The ethylpyridine guests interact with molecule of **2** only via weak CH···N hydrogen bond from the host pyridyl CH groups. This process is reminiscent of gel-like characteristics where the solid network of **2** traps the solvent molecules rendering them immobile. Experiments were carried out in an attempt to replace the 4-ethylpyridine with isoniazid. A series of crystallisation experiments with varying concentrations of isoniazid in a 1 wt. % solution of **2** in 4-ethylpyridine were investigated however only crystals of **2**·4-ethylpyridine resulted.

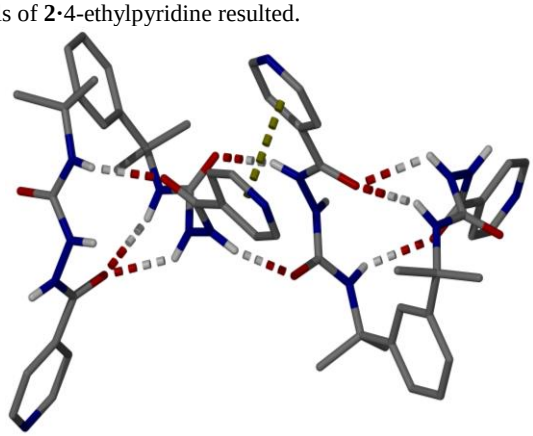

Figure 11. Hydrogen bonding interactions observed between neighbouring molecules of **2** in the asymmetric unit of **2**·4-ethylpridine. The yellow dashed line highlights a π-stacking interaction. Solvent molecules and hydrogen atoms not involved in hydrogen bonding interactions are omitted for clarity.

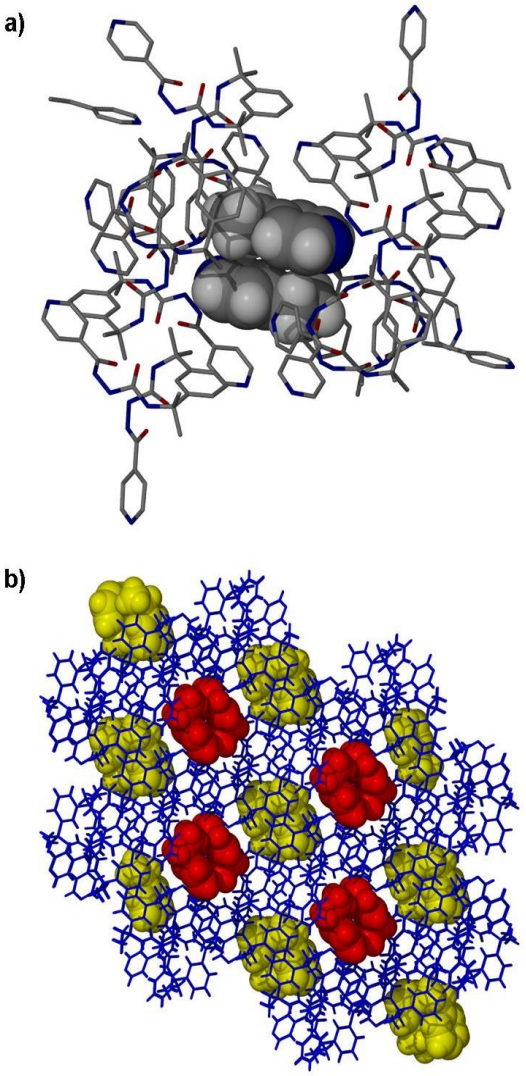

Figure 12. a) Partial space filling representation of encapsulated 4-ethylpyridine guest molecules in **2**·4-ethylpridine. Guest molecules are highlighted as space filling representation. All hydrogen atoms are omitted for clarity except for those on the highlighted guest molecules. b) Crystal packing in **2**·4-ethylpridine. Molecules of **2** are shown in blue and pairs of 4-ethylpyridine molecules are highlighted in either red and yellow space filling representation showing their isolation.

Conclusion

We have shown that it is possible to design a tailored gelator for isoniazid through a relatively simple one step synthetic procedure. Gel phase crystallisation of isoniazid versus solution phase crystallisation produces some significant differences in crystal habit and crystal size. Crystals can also be grown in a gel based on a solvent that typically does not produce any crystalline material. In one case crystallization is conveniently accompanied by gel collapse, facilitating crystal recovery. Despite these differences, both supramolecular gel and microemulsion crystallization methods give rise to the one known polymorph of isoniazid that is also obtained from

 This journal is © The Royal Society of Chemistry 2012

solution, reinforcing the view that this compound only crystallises in one non-solvated polymorphic form. The sterically hindered isoniazid derivative **2** does not form gels. Its various crystal structures give an insight into the factors which prevent gelation as a result of competing hydrogen bonding interactions and steric interference from the bulky spacer group. The **2**·4-ethylpyridine co-crystal structure is interesting from the point of view of building insight into the aggregation of drug-like molecule close to the surface of LMWGs. While this work has not expanded the experimental solid form landscape of isoniazid, this combined gel and microemulsion strategy represents a potentially powerful polymorph discovery tool in less well explored and potentially polymorphic systems.

Experimental

Synthesis

Compound **1**: Isoniazid (0.5 g, 3.65 mmol) was added to a solution of 4,4-methylenebis(2,6-diethylaniline) (0.66 g, 1.82 mmol) in chloroform:ethanol (15 mL:1.5 mL) and triethylamine (1 mL, 7.17 mmol) to give a solution that was heated under reflux for 24 h. A precipitated formed which was filtered and washed with $CHCl_3$ to give **1** as a white solid (0.98 g, 1.54 mmol, 84%). ^{1}H NMR (400 MHz, DMSO-d_6) δ 10.56 (s, 2H, NH), 8.78 – 8.69 (m, 4H, ArH), 8.20 (s, 2H, NH), 7.98 (s, 2H, NH), 7.83 (d, ^3J = 5.1 Hz, 4H, ArH), 6.94 (s, 4H, ArH), 3.84 (d, J = 6.1 Hz, 2H, CH_2), 2.57 – 2.46 (m, 8H, CH_2CH_3), 1.07 (d, J = 7.4 Hz, 12H, CH_2CH_3); ^{13}C{^{1}H} NMR (400 MHz, DMSO-d_6) δ 165.38 (C=O), 150.47 (ArC), 142.42 (ArC), 140.16 (ArC), 132.18 (ArC), 126.38 (ArC), 121.94 (ArC), 46.13 (CH_2), 24.68 (CH_2CH_3), 15.35 (CH_2CH_3). ESI-MS M+H$^+$ *m/z* 637.8.

Compound **2**: Isoniazid (0.51 g, 3.72 mmol) was added to a solution of 1,3-bis(1-isocyanato-1-methylethyl)benzene (0.42 mL, 1.82 mmol) in chloroform:ethanol (15 mL:1.5 mL). and triethylamine (1 mL, 7.17 mmol) to give a solution that was heated under reflux for 24 h. A precipitated formed which was filtered and washed with $CHCl_3$ to give **2** as a white solid (0.92 g, 1.77 mmol, 95%) ^{1}H NMR (400 MHz, DMSO-d_6) δ 10.46 (d, ^3J = 2.8 Hz, 2H, NH), 8.76 – 8.70 (m, 4H, ArH), 7.92 (d, ^3J = 2.8 Hz, 2H, NH), 7.80 – 7.73 (m, 4H, ArH), 7.44 (q, ^3J = 1.4 Hz, 1H, ArH), 7.25 – 7.18 (m, 3H, ArH), 6.77 (s, 2H, NH), 1.59 (s, 12H, CH_3); ^{13}C{^{1}H} NMR (400 MHz, DMSO-d_6) δ 165.14 (C=O), 157.22 (C=O), 150.73 (ArC), 148.23 (ArC), 140.08 (ArC), 127.74 (ArC), 122.94 (ArC), 121.75 (ArC), 55.31 (CCH_3), 30.44 (CCH_3). ESI-MS M–H$^+$ *m/z* 517.2.

Scanning Electron Microscopy

SEM samples were dried in air at room temperature for 2 days, coated with 3 nm of chromium using a Cressington 328 Ultra High Resolution EM Coating System, and imaged using an FEI Helios NanoLab DualBeam microscope in immersion mode, with typical beam settings of 1.5 kV and 0.17 nA.

Single crystal X-ray diffraction

Single crystal data for **2**, **2**·H_2O, **2**·2 propan-2-ol, **2**·2 cyclohexanone were collected at 120.0(2) K on a Bruker D8Venture diffractometer (PHOTON-100 CMOS detector, IμS-microsource, focusing mirrors, MoKα, λ = 0.71073Å) and processed using Bruker APEX-II software. The temperature of the samples was maintained by the Cryostream (Oxford Cryosystems) open-flow nitrogen cryostat. The data for 2_butanol and **2**·4-ethylpyridine were collected at 120K on a Rigaku Saturn 724+ diffractometer at station I19 of the Diamond Light Source synchrotron (undulator, λ = 0.6889 Å, ω-scan, 1.0°/frame) and processed using Bruker APEXII software.

Crystals of **2** were prepared by allowing a propan-1-ol solution of the sample to slowly evaporate. Crystal data for **2**, $C_{26}H_{30}N_8O_4$, M = 518.58, 0.35 × 0.27 × 0.15 mm^3, tetragonal, space group $I\bar{4}2d$ (No. 122), a = b = 15.8133(5), c = 20.5773(8) Å, V = 5145.6(4) Å^3, Z = 8, D_c = 1.339 g/cm^3, μ = 0.094 mm^{-1}, F_{000} = 2192, 41617 reflections collected, 3749 unique (R_{int} = 0.0416). Final GOOF = 1.040, R_1 = 0.0329 (3480 reflections with I >2σ(I)), wR_2 = 0.0814, (all data, refinement on F^2), 233 parameters, 0 restraints.

Crystals of **2**·H_2O were prepared by allowing a water solution of the sample to slowly evaporate. Crystal data for **2**·H_2O, $C_{26}H_{32}N_8O_5$, M = 536.60, 0.094 × 0.161 × 0.218 mm^3, orthorhombic, space group $P2_12_12_1$ (No. 19), a = 9.0337(7), b = 14.7317(14), c = 19.8607(15) Å, V = 2643.1(4) Å^3, Z = 4, D_c = 1.355 g/cm^3, μ = 0.097 mm^{-1} F_{000} = 1136, 27044 reflections collected, 7018 unique (R_{int} = 0.1001). Final GOOF = 1.020, R_1 = 0.0723 (5290 reflections with I >2σ(I)), wR_2 = 0.1782, (all data, refinement on F^2), 359 parameters, 0 restraints.

Crystals of **2**·2 propan-2-ol were prepared by allowing a propan-2-ol solution of the sample to slowly evaporate. Crystal data for **2**·2 propan-2-ol, $C_{32}H_{44}N_8O_6$, M = 636.75, 0.105 × 0.145 × 1.016 mm^3, orthorhombic, space group *Pbca* (No. 61), a = 17306(2), b = 16.8727(19), c = 23.268(3) Å, V = 6794.3(15) Å^3, Z = 8, D_c = 1.245 g/cm^3, μ = 0.088 mm^{-1}, F_{000} = 2720, 57136 reflections collected, 7413 unique (R_{int} = 0.2469). Final GOOF = 1.015, R_1 = 0.0868 (3777 reflections with I >2σ(I)), *wR2* = 0.2169, (all data, refinement on F^2), 425 parameters, 0 restraints.

Crystals of **2**·4-ethylpyridine were prepared by allowing a 4-ethylpyridine solution of the sample to slowly evaporate. Crystal data for **2**·4-ethylpyridine, $C_{66}H_{78}N_{18}O_8$, M = 625.73, 0.398 × 0.081 × 0.060 mm^3, triclinic, space group P-1 (No. 2), a = 13.3968(8), b = 16.0797(6), c = 16.7219(8) Å, α = 84.489(4), β = 67.608(5), γ = 82.921(4)°, V = 3300.5(3) Å^3, Z = 2, D_c = 1.259 g/cm^3, μ = 0.088 mm^{-1} ,F_{000} = 1328, 37133 reflections collected, 17743 unique (R_{int} = 0.0535). Final GOOF = 1.035, R_1 = 0.0603 (12650 reflections with I >2σ(I)), wR_2 = 0.2320, (all data, refinement on F^2), 842 parameters, 0 restraints.

Crystals of **2**·2 cyclohexanone were prepared by allowing a cyclohexanone solution of the sample to slowly evaporate. Crystal data for **2**·2 cyclohexanone: $C_{38}H_{50}N_8O_6$, M = 1429.72, 0.30 × 0.16 × 0.12 mm^3, monoclinic, space group $P2_1/c$ (No. 14), a = 16.641(3), b = 16.911(3), c = 26.532(4) Å, β = 92.145(5)°, V = 7461(2) Å^3, Z = 8, D_c = 1.273 g/cm^3, μ = 0.089 mm^{-1}, F_{000} = 3056, 660605 reflections collected, 14706 unique (R_{int} = 0.1263). Final GOOF = 1.164, R_1 = 0.1197 (7681 reflections with I >2σ(I)), wR_2 = 0.2607 (all data, refinement on F^2), 946 parameters, 0 restraints.

Conflicts of interest

There are no conflicts of interest to declare

Acknowledgements

We thank the Engineering and Physical Sciences Research Council for funding grant EP/J013021/1. We are also grateful to the Diamond Light Source for an award of instrument time on the Station I19, grant MT8682.

Notes and references

[a] Department of Chemistry, Durham University, South Road, Durham, DH1 3LE, UK.

E-mail: jon.steed@durham.ac.uk; Fax: +44(0)191 384 4737;

Tel: +44 (0)191 334 2085

[b] Department of Applied Sciences, Northumbria University, Newcastle upon Tyne, NE1 8ST, UK.

† Electronic Supplementary Information (ESI) available: Gelation test table, NMR and mass spectroscopic data and addition photographs. See DOI: 10.1039/c000000x/. Crystallographic data has been deposited with the CCDC as deposition numbers 1817000-1817002, 1817004-1817006.

1. W. C. McCrone, in *Physics and Chemistry of the Organic Solid State*, eds. D. Fox, M. M. Labes and A. Weissberger, Interscience Publishers, London, 1965, vol. 2, pp. 725.
2. S. L. Price, *Chem. Soc. Rev.*, 2014, **43**, 2098.
3. U. J. Griesser, in *Polymorphism: In the Pharmaceutical Industry*, ed. R. Hilfiker, Wiley-VCH, Weinheim, 2006, p. 220.
4. J. C. Hanson, N. Camerman and A. Camerman, *J. Med. Chem.*, 1981, **24**, 1369.
5. J. Suarez, K. Ranguelova, A. A. Jarzecki, J. Manzerova, V. Krymov, X. B. Zhao, S. W. Yu, L. Metlitsky, G. J. Gerfen and R. S. Magliozzo, *J. Biol. Chem.*, 2009, **284**, 7017.
6. L. H. Jensen, *J. Am. Chem. Soc.*, 1954, **76**, 4663.
7. T. N. Bhat, T. P. Singh and M. Vijayan, *Acta Crystallogr. Sect. B*, 1974, **30**, 2921.
8. A. Lemmerer, *CrystEngComm*, 2012, **14**, 2465.
9. G. Rajalakshmi, V. R. Hathwar and P. Kumaradhas, *Acta Crystallogr. Sec. B.*, 2014, **70**, 331.
10. B. Swapna, D. Maddileti and A. Nangia, *Cryst. Growth Des.*, 2014, **14**, 5991.
11. I. Sarcevica, L. Orola, M. V. Veidis, A. Podjaya and S. Belyakov, *Cryst. Growth Des.*, 2013, **13**, 1082.
12. P. Grobelny, A. Mukherjee and G. R. Desiraju, *CrystEngComm*, 2011, **13**, 4358.
13. S. Cherukuvada and A. Nangia, *CrystEngComm*, 2012, **14**, 2579.
14. A. Lemmerer, J. Bernstein and V. Kahlenberg, *CrystEngComm*, 2010, **12**, 2856.
15. A. Lemmerer, J. Bernstein and V. Kahlenberg, *CrystEngComm*, 2011, **13**, 55.
16. S. Aitipamula, A. B. H. Wong, P. S. Chow and R. B. H. Tan, *CrystEngComm*, 2013, **15**, 5877.
17. H. G. Brittain, *Cryst. Growth Des.*, 2012, **12**, 1046.
18. J. A. Foster, M.-O. M. Piepenbrock, G. O. Lloyd, N. Clarke, J. A. K. Howard and J. W. Steed, *Nature Chem.*, 2010, **2**, 1037.
19. D. K. Kumar and J. W. Steed, *Chem. Soc. Rev.*, 2014, **43**, 2080.
20. J. A. Foster, K. K. Damodaran, A. Maurin, G. M. Day, H. P. G. Thompson, G. J. Cameron, J. C. Bernal and J. W. Steed, *Chem. Sci.*, 2017, **8**, 78.
21. L. Kaufmann, S. R. Kennedy, C. D. Jones and J. W. Steed, *Chem. Commun.*, 2016, **52**, 10113.
22. C. Ruiz-Palomero, S. R. Kennedy, M. L. Soriano, C. D. Jones, M. Valcarcel and J. W. Steed, *Chem. Commun.*, 2016, **52**, 7782.
23. F. Aparicio, E. Matesanz and L. Sánchez, *Chem. Commun.*, 2012, **48**, 5757.
24. J. Buendia, E. Matesanz, D. K. Smith and L. Sanchez, *CrystEngComm*, 2015, **17**, 8146.
25. L. A. Estroff, L. Addadi, S. Weiner and A. D. Hamilton, *Org. Biomol. Chem.*, 2004, **2**, 137.
26. P. Terech and R. G. Weiss, *Chem. Rev.*, 1997, **97**, 3133.
27. Z. L. Wang Xiu-Feng, Liu Ming-Hua, *Acta Phys. -Chim. Sin.*, 2016, **32**, 227.
28. C. D. Jones and J. W. Steed, *Chem. Soc. Rev.*, 2016, **45**, 6546.
29. P. Dastidar, S. Ganguly and K. Sarkar, *Chem. Asian J.*, 2016, **11**, 2484.
30. Y. Lan, M. G. Corradini, R. G. Weiss, S. R. Raghavan and M. A. Rogers, *Chem. Soc. Rev.*, 2015, **44**, 6035.
31. S. L. James, G. O. Lloyd and J. Y. Zhang, *Crystengcomm*, 2015, **17**, 7976.
32. R. G. Weiss, *J. Am. Chem. Soc.*, 2014, **136**, 7519.
33. A. Y.-Y. Tam and V. W.-W. Yam, *Chem. Soc. Rev.*, 2013, **42**, 1540.
34. A. Dawn, K. S. Andrew, D. S. Yufit, Y. X. Hong, J. P. Reddy, C. D. Jones, J. A. Aguilar and J. W. Steed, *Cryst. Growth Des.*, 2015, **15**, 4591.
35. P. Dastidar, *Chem. Soc. Rev.*, 2008, **37**, 2699.
36. M. Suzuki, Y. Nakajima, M. Yumoto, M. Kimura, H. Shirai and K. Hanabusa, *Org. Biomol. Chem.*, 2004, **2**, 1155.
37. M. de Loos, A. G. J. Ligtenbarg, J. van Esch, H. Kooijman, A. L. Spek, R. Hage, R. M. Kellogg and B. L. Feringa, *Eur. J. Org. Chem.*, 2000, 3675.
38. C. Chen, C. E. Nicholson, H. E. Ramsey and S. J. Cooper, *Cryst. Growth Des.*, 2015, **15**, 1060.
39. C. E. Nicholson, C. Chen, B. Mendis and S. J. Cooper, *Cryst. Growth Des.*, 2011, **11**, 363.
40. J. Liu, C. E. Nicholson and S. J. Cooper, *Langmuir*, 2007, **23**, 7286.
41. C. Chen, O. Cook, C. E. Nicholson and S. J. Cooper, *Cryst. Growth Des.*, 2011, **11**, 2228.
42. J. S. Foster, J. M. Zurek, N. M. S. Almeida, W. E. Hendriksen, V. A. A. le Sage, V. Lakshminarayanan, A. L. Thompson, R. Banerjee, R. Eelkema, H. Mulvana, M. J. Paterson, J. H. van Esch and G. O. Lloyd, *J. Am. Chem. Soc.*, 2015, **137**, 14236.
43. A. M. Todd, K. M. Anderson, P. Byrne, A. E. Goeta and J. W. Steed, *Cryst. Growth Des.*, 2006, **6**, 1750.
44. A. Cayuela, S. R. Kennedy, M. L. Soriano, C. D. Jones, M. Valcarcel and J. W. Steed, *Chem. Sci.*, 2015, **6**, 6139.
45. G. Cravotto and P. Cintas, *Chem. Soc. Rev.*, 2009, **38**, 2684.
46. M.-O. M. Piepenbrock, N. Clarke and J. W. Steed, *Soft Matter*, 2010, **6**, 3541.
47. M. O. M. Piepenbrock, G. O. Lloyd, N. Clarke and J. W. Steed, *Chem. Commun.*, 2008, 2644.
48. K. M. Steed and J. W. Steed, *Chem. Rev.*, 2015, **115**, 2895.
49. P. Byrne, D. R. Turner, G. O. Lloyd, N. Clarke and J. W. Steed, *Cryst. Growth Des.*, 2008, **8**, 3335.
50. P. Byrne, G. O. Lloyd, L. Applegarth, K. M. Anderson, N. Clarke and J. W. Steed, *New J. Chem.*, 2010, **34**, 2261.
51. R. Bishop and M. L. Scudder, *Cryst. Growth Des.*, 2009, **9**, 2890.
52. L. A. Estroff and A. D. Hamilton, *Chem. Rev.*, 2004, **104**, 1201.
53. J. H. van Esch, F. Schoonbeek, M. de Loos, H. Kooijman, A. L. Spek, R. M. Kellogg and B. L. Feringa, *Chem. Eur. J.*, 1999, **5**, 937.
54. M. Pauchet, T. Morelli, S. Coste, J.-J. Malandain and G. Coquerel, *Cryst. Growth Des.*, 2006, **6**, 1881.

 This journal is © The Royal Society of Chemistry 2012

For Table of Contents use only

A tailored supramolecular gel and microemulsion crystallization strategy has been applied to isoniazid crystal screening.